MOLECULAR AND CELLULAR BIOLOGY, Jan. 2006, p. 131–139 Vol. 26, No. 1
0270-7306/06/$08.00+0 doi:10.1128/MCB.26.1.131–139.2006

Alternative Pathways for the Repair of RAG-Induced DNA Breaks

David M. Weinstock[1] and Maria Jasin[2]*

Department of Medicine[1] and Molecular Biology Program,[2] Memorial Sloan-Kettering Cancer Center, 1275 York Avenue, New York, New York 10021

Received 15 May 2005/Returned for modification 13 June 2005/Accepted 13 October 2005

RAG1 and RAG2 cleave DNA to generate blunt signal ends and hairpin coding ends at antigen receptor loci in lymphoid cells. During V(D)J recombination, repair of these RAG-generated double-strand breaks (DSBs) by the nonhomologous end-joining (NHEJ) pathway contributes substantially to the antigen receptor diversity necessary for immune system function, although recent evidence also supports the ability of RAG-generated breaks to undergo homology-directed repair (HDR). We have determined that RAG-generated chromosomal breaks can be repaired by pathways other than NHEJ in mouse embryonic stem (ES) cells, although repair by these pathways occurs at a significantly lower frequency than NHEJ. HDR frequency was estimated to be ≥40-fold lower than NHEJ frequency for both coding end and signal end reporters. Repair by single-strand annealing was estimated to occur at a comparable or lower frequency than HDR. As expected, V(D)J recombination was substantially impaired in cells deficient for the NHEJ components Ku70, XRCC4, and DNA-PKcs. Concomitant with decreased NHEJ, RAG-induced HDR was increased in each of the mutants, including cells lacking DNA-PKcs, which has been implicated in hairpin opening. HDR was increased to the largest extent in *Ku70*$^{-/-}$ cells, implicating the Ku70/80 DNA end-binding protein in regulating pathway choice. Thus, RAG-generated DSBs are typically repaired by the NHEJ pathway in ES cells, but in the absence of NHEJ components, a substantial fraction of breaks can be efficiently channeled into alternative pathways in these cells.

Nonhomologous end-joining (NHEJ) of DNA double-strand breaks (DSBs) created by the RAG recombinase during V(D)J recombination generates a substantial portion of the diversity found in antigen receptors (6, 11). The RAG recombinase, composed of the RAG1 and RAG2 proteins, initiates recombination by introducing nicks at recombination signal sequences (RSS elements), each composed of conserved heptamer and nonamer sequences separated by a nonconserved spacer of either 12 bp or 23 bp. Through a transesterification reaction the nicks become converted to DSBs, resulting in two hairpin coding ends and two blunt signal ends. The signal ends undergo precise joining, whereas the hairpin coding ends undergo further processing prior to joining, resulting in a diverse set of junctions. In addition to the cleavage reaction, the RAG proteins participate in end processing and joining, possibly by maintaining the ends in a postcleavage complex, which serves as a scaffold to facilitate repair (1, 14, 38, 48, 52).

The proteins involved in NHEJ of RAG-induced DSBs during V(D)J recombination include the DNA end-binding protein Ku70/80, the Ser/Thr kinase DNA-PKcs, the XRCC4/ligase IV complex, and the Artemis protein, which has endonuclease activity (6, 24). Mutant cell lines for each of these NHEJ proteins have severely impaired formation of coding joints during V(D)J recombination, whereas only Ku70/80- and XRCC4/ligase IV-deficient cells are markedly impaired for signal joint formation (2, 8, 12, 23, 40, 46). These proteins are also involved in the repair of DSBs generated by ionizing radiation and other DNA-damaging agents, since mutant cell lines are hypersensitive to these agents (15, 40). In addition, mutant cells can exhibit spontaneous chromosomal rearrangements, in some cases leading to oncogenic translocations in mice (7). NHEJ is not totally abrogated in cells deficient for these components, however, since efficient joining of DSBs in plasmids (see, e.g., reference 50) and a low level of V(D)J recombination are observed. In addition, sequence analysis of oncogenic translocation junctions derived from NHEJ mutant mice indicates repair by nonhomologous processes (4, 53). Thus, one or more poorly defined, alternative NHEJ pathways exist in cells, which may be prone to causing rearrangements. To distinguish NHEJ involving these alternative pathways from NHEJ involving the components necessary for robust V(D)J recombination, the latter pathway has often been termed "classical" NHEJ.

NHEJ involves little or no sequence homology at the DSB. Mammalian cells also efficiently repair DSBs by homologous recombination, also termed homology-directed repair (HDR), as demonstrated by studies using the rare-cutting endonuclease I-SceI (22). Central to HDR is a DNA strand exchange involving the invasion of single-stranded DNA into a homologous duplex DNA, a reaction that is promoted by the Rad51 protein (33, 45). HDR is generally considered to be a precise form of repair, because it can restore the original sequence of a damaged chromosome by using a homologous sequence, preferably the sister chromatid (16), as a template for repair synthesis. This contrasts with NHEJ, in which joining may be imprecise (15, 24). In addition to HDR, a second pathway involving sequence homology, termed single-strand annealing (SSA), can mediate repair if sequence repeats are located near the DSB (33, 45). Like HDR, SSA involves single strands formed by resection at a DSB, but, unlike HDR, SSA occurs by the annealing of the single strands rather than strand invasion.

* Corresponding author. Mailing address: Molecular Biology Program, Memorial Sloan-Kettering Cancer Center, 1275 York Avenue, New York, NY 10021. Phone: (212) 639-7438. Fax: (212) 717-3317. E-mail: m-jasin@ski.mskcc.org.

We investigated repair pathway choice of RAG-generated chromosomal breaks using a mouse embryonic stem (ES) cell system and NHEJ-deficient cell lines. Lee and colleagues have recently demonstrated that the RAG proteins can induce HDR at RSS elements (17). We now extend these studies and find that HDR is induced by expression of full-length RAG proteins using either a coding end or signal end chromosomal reporter and that RAG-induced HDR requires the Rad51 strand exchange protein. RAG-generated breaks can also be repaired by SSA. However, HDR and SSA occur at low frequencies compared with NHEJ [i.e., V(D)J recombination]. In addition, the frequency of HDR is substantially higher in *Ku70*$^{-/-}$, *DNA-PKcs*$^{-/-}$, and *XRCC4*$^{-/-}$ ES cell lines, with the highest frequency in *Ku70*$^{-/-}$ cells. These results indicate that classical NHEJ factors not only mediate repair of RAG-generated breaks in these cells but also channel repair into V(D)J recombination, thereby suppressing repair by HDR.

MATERIALS AND METHODS

DNA manipulations and cell transfections. The cDNAs for full-length RAG1, RAG2, and RAG2-T490A were cloned from pcRAG-1, pcRAG-2 (25), and pcRAG-2 T490A (21) into the pCAGGS expression vector (29) to create the pCAGGS-RAG1, pCAGGS-RAG2, and pCAGGS-RAG2-T490A vectors, respectively. The targeting vector hprtDRGFP-NICE was created by cloning a fragment containing a 12-bp spacer RSS (5′-CACAGTGCTACAGACTGGAA CAAAAACC-3′), NsiI site, BstBI site, and 23-bp spacer RSS (5′-GGTTTTTG TACAGCCAGACAGTGGAGTACTACCACTGTG-3′) (13) into the unique I-SceI site in the hprtDRGFP targeting vector (35), such that the RSS elements are oriented to produce chromosomal coding ends upon RAG1/RAG2 cleavage. The DRGFP-CE substrate was created by cloning a 333-bp intronic sequence from the human β-globin gene into the NsiI and BstBI sites in DRGFP-NICE to expand the distance between the RSS elements. DRGFP-SE is identical to DRGFP-CE, except the RSS elements are oriented to produce chromosomal signal ends. DRGFP-CE, DRGFP-SE, and DRGFP-NICE were targeted to the hypoxanthine phosphoribosyltransferase gene (*hprt*) locus in wild-type and NHEJ mutant ES cells (9, 10, 12), as previously described (36). Targeting was confirmed by Southern blotting (36). In addition to targeted clones, *Ku70*$^{-/-}$ clones with a single copy of DRGFP-CE randomly integrated into the genome (*hprt*$^{+}$/*puro*^{R}) were also isolated and were used to analyze individual repair products after RAG1/RAG2 cleavage.

For HDR assays, 0.8 μg of empty vector (pCAGGS), the I-SceI expression vector pCBASce (39), or pCAGGS-RAG1 and pCAGGS-RAG2 was transfected into ES cells in 24-well plates using Lipofectamine 2000 (Invitrogen, Inc.), according to the manufacturer's instructions. The same quantities of expression vectors for Ku70 and Rad51-K133R (42) and pCAGGS-RAG2-T490A were used in cotransfection experiments. Flow-cytometric analysis was performed on a Becton Dickinson FACScan 96 h after transfection, as described previously (37).

PCR and sequencing. A combined PCR-Southern blotting strategy was used to examine RAG-induced NHEJ, HDR, and SSA. Genomic DNA was isolated 7 days after transfection and used as the template for PCR with previously described primers (31), except that amplification was performed for 22 cycles with a 1 min 20 s elongation time. The products were separated on a 1.5% agarose gel, transferred to a nylon membrane, and probed with a ^{32}P-labeled fragment from DR-GFP, which was cut with HindIII/BamHI, as previously described (31). Quantification was performed using ImageJ software (rsb.info.nih.gov/ij/).

To analyze individual repair products, genomic DNA was digested with NdeI and MfeI, which cleave within the sequence between the RSS elements, and then 0.4 μg was used as the template for PCR with primers DRGFP1 and DRGFP2, as previously described (35). The PCR product (5 μl) was subjected to TOPO TA cloning (Invitrogen, Inc.) and transformed into Top10-competent *Escherichia coli*. Individual colonies were isolated and analyzed by BcgI digestion and sequencing (Bio Resource Center, Cornell University, Ithaca, NY).

RESULTS

HDR induced by RAG recombinase. To determine the frequency of RAG-induced HDR, we modified our green fluorescence protein (GFP)-based reporter, DR-GFP, to contain RSS elements. DR-GFP contains the cleavage site for the rare-cutting I-SceI endonuclease within one of two defective *GFP* repeats (Fig. 1A) (37). We inserted two RSS elements—one containing a 12-bp spacer and the other containing a 23-bp spacer—into the I-SceI site of DR-GFP, with the RSS elements separated by 333 bp of intronic sequence derived from the human β-globin gene. In DRGFP-SE, the RSS elements are oriented such that RAG-mediated cleavage will produce two blunt signal ends (SE) and excise a 333-bp fragment with two hairpin coding ends. In DRGFP-CE, the RSS elements are in the opposite orientation, such that RAG-mediated cleavage produces two hairpin coding ends (CE) and excises a 400-bp fragment with blunt signal ends. After cleavage, DNA ends repaired by HDR through a noncrossover gene conversion, the most frequent type of HDR event, will restore a functional *GFP* gene.

We introduced the HDR reporters into mouse ES cells. Colonies that were *hprt*$^{-}$/puro^{R} were selected, as each reporter is flanked by *hprt* sequences to target the reporters to the *hprt* locus (35) and, as well, contains the selectable puromycin resistance gene (*puro*^{R}) between the *GFP* repeats (Fig. 1A). Correct targeting was confirmed by Southern hybridization (Fig. 1B). With the HDR reporters integrated at the *hprt* locus in each of the cell lines, possible position effects on cleavage or repair that may arise from random integration should be abrogated (35).

In the absence of RAG1/RAG2 expression, GFP-positive (GFP^{+}) cells were rarely observed: in cells containing the DRGFP-SE and DRGFP-CE reporters, 0.001 and 0.002% of cells, respectively, were measured by flow cytometry to be GFP^{+}. However, after transient expression of full-length RAG1/RAG2 into the appropriate cell lines, GFP^{+} cells were detected at significantly higher frequencies, indicating HDR (Fig. 1C). An average of 0.026% of cells obtained from cells containing the DRGFP-SE reporter were GFP^{+}, and 0.073% of cells obtained from cells containing the DRGFP-CE reporter were GFP^{+}, an ~30-fold-higher level than that in the absence of RAG1/RAG2 expression (Fig. 1D). For comparison, approximately 1.8% of cells obtained after I-SceI expression from cells containing the DR-GFP reporter were GFP^{+} (Fig. 1C), similar to our previous results with this reporter (35). Thus, 70-fold (DRGFP-SE)- and 25-fold (DRGFP-CE)-lower rates of HDR were obtained with RAG1/RAG2 expression compared with I-SceI expression using similar reporter substrates. The recovery of GFP^{+} cells was dependent on the HDR protein Rad51, as expression of a mutant Rad51 protein (Rad51-K133R), which can interfere with HDR in a dominant manner (42, 44), reduced the number of GFP^{+} cells to background levels (0.001%) (Fig. 1C and D).

The RAG-induced GFP^{+} cells formed a distinct population of green fluorescent cells by flow cytometry and were obtained at a substantially higher frequency than in the absence of RAG1/RAG2 expression. However, given their low frequency, we verified that they arose from HDR by enriching for the GFP^{+} population by flow sorting (Fig. 1C). Genomic DNA was isolated from the sorted populations and confirmed to contain the expected sequence for a functional *GFP* gene (data not shown).

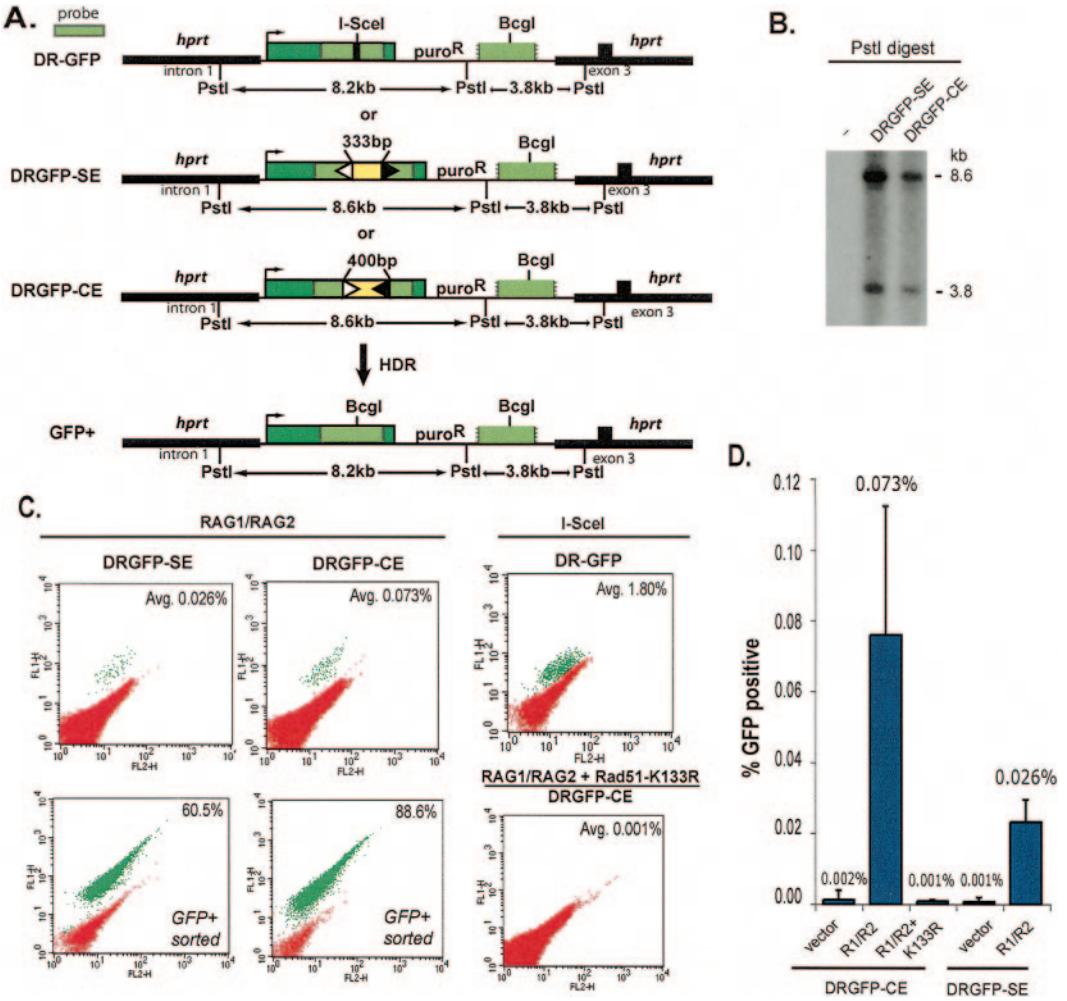

FIG. 1. Homology-directed repair at RAG-generated breaks. A. HDR reporters for RAG-generated DSBs were designed based on the previously published DR-GFP reporter (37) for the repair of I-SceI endonuclease-generated DSBs. The DRGFP-SE (signal end) and DRGFP-CE (coding end) reporters have two RSS elements, one having a 12-bp spacer (white triangle) and the other a 23-bp spacer (black triangle), which interrupt a *GFP* gene (green box). The RSS elements are separated by 333 bp (yellow box) and, when cleaved by the RAG proteins, generate a *GFP* gene with either signal ends (DRGFP-SE) or coding ends (DRGFP-CE). DSB repair by a noncrossover gene conversion with the downstream 5′- and 3′-truncated *GFP* gene results in a functional *GFP* gene. Unlike DRGFP-CE, gene conversion at DRGFP-SE requires end processing to remove the RSS elements (see also Fig. 2A). B. Southern analysis demonstrating targeting of the DRGFP-SE and DRGFP-CE reporters to the *hprt* locus in mouse ES cells. Genomic DNA was digested with PstI, which cleaves once in the reporter targeting fragment. Fragments of 8.6 and 3.8 kb are obtained from $hprt^{-}$/$puro^{R}$ cells that are appropriately targeted. Lane −, negative control. C. Flow-cytometric analysis of ES cells containing the HDR reporters at the *hprt* locus after expression of full-length RAG1 and RAG2 in cells containing DRGFP-SE or DRGFP-CE (in the latter case with Rad51-K133R where indicated) or after I-SceI expression in cells containing DR-GFP. The percentage of GFP^{+} cells obtained from >50,000 analyzed cells is indicated (average from three or more experiments). GFP^{+} cells arising from RAG1/RAG2 expression were also enriched by flow sorting. D. Frequency of GFP^{+} cells by flow cytometry in ES cells containing the HDR reporters after transient transfection of either empty vector, full-length RAG1 and RAG2 (R1/R2), or full-length RAG1 and RAG2 and Rad51-K133R (K133R). Error bars indicate 1 standard deviation from the mean.

HDR is a small fraction of overall repair occurring at RAG-generated breaks. The low absolute frequency of HDR induced by the RAG proteins compared with I-SceI could result either from infrequent HDR at RAG-generated DSBs compared with NHEJ or from a low efficiency of cleavage at the integrated RSS elements. We sought to determine, therefore, the amount of V(D)J recombination at the RSS elements in our reporters. We used a PCR primer set that amplifies the unrearranged DRGFP-SE or DRGFP-CE reporter to produce a 1.5-kb fragment and products resulting from either NHEJ or HDR, both of which would produce a 1.1-kb fragment (SA-F and SA-R1; Fig. 2A). Since the smaller fragment from repair amplifies more efficiently than the larger fragment from the unrearranged reporter, we created a standard curve for comparing the observed ratio of the fragments and the expected ratio by performing PCR on various dilutions of DNA from untransfected cells containing the DR-GFP reporter–which would give rise to a 1.1-kb fragment—into DNA from untransfected cells containing the DRGFP-CE reporter (Fig. 2B).

In the absence of RAG expression, only the 1.5-kb fragment from the unrearranged reporters was detected (Fig. 2B). In contrast, transient expression of RAG1/RAG2 produced both

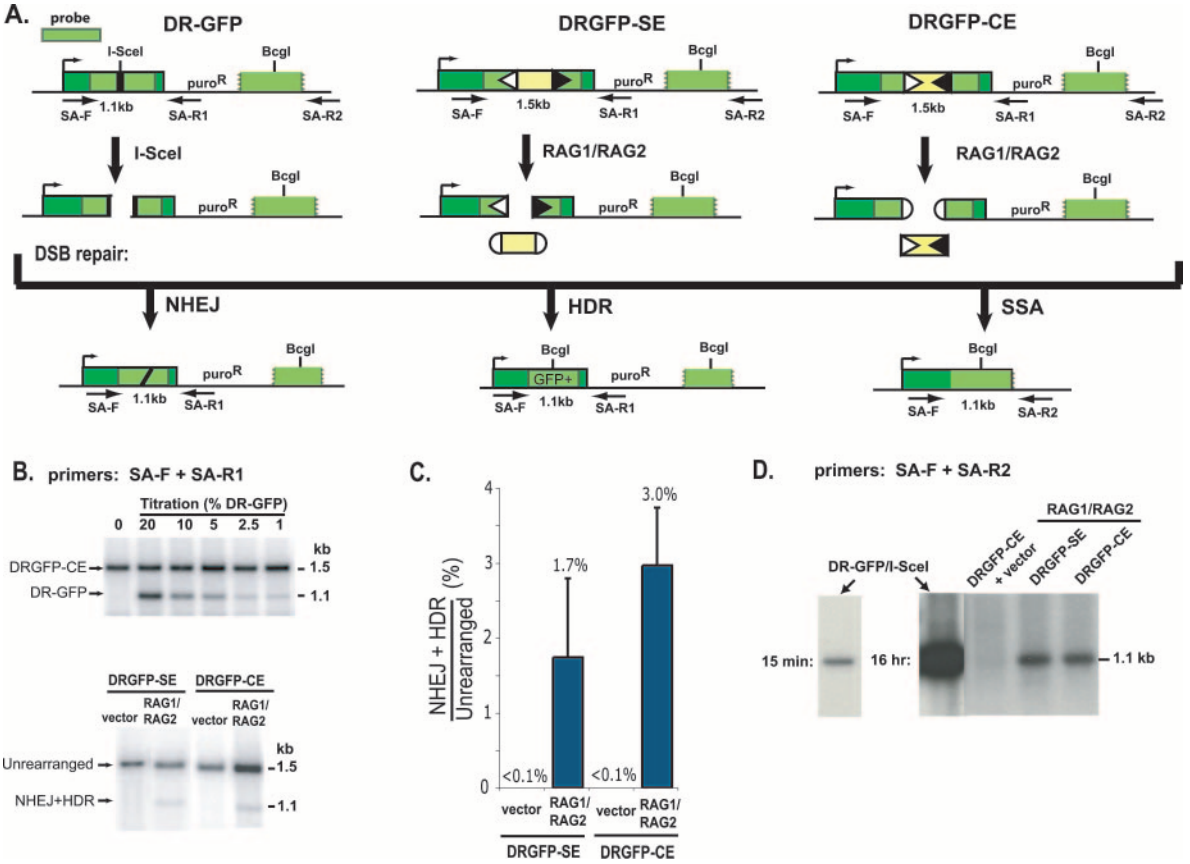

FIG. 2. Multiple repair pathways for RAG-generated breaks. A. DSB formation by I-SceI or RAG1/RAG2 and repair by NHEJ, HDR, and SSA at the HDR reporter substrates. Only HDR results in a functional *GFP* gene, although all three pathways can be assayed with PCR using the indicated primer pairs. Primers SA-F and SA-R1 are used to assay NHEJ and HDR, giving rise to a 1.1-kb fragment, with the amount of HDR determined by flow cytometry for GFP^+ cells and the amount of NHEJ inferred by subtracting the amount of HDR. Primers SA-F and SA-R2 are used to assay SSA, giving rise to a 1.1-kb fragment. Symbols are as in Fig. 1. B. RAG-generated DSBs are primarily repaired by NHEJ. Upper panel, PCR titration using various dilutions of DNA from untransfected cells containing the DR-GFP reporter, which gives rise to a 1.1-kb fragment, into DNA from untransfected cells containing the DRGFP-CE reporter, which gives rise to a 1.5-kb fragment; lower panel, experimental samples from cells containing the DRGFP-SE or DRGFP-CE substrates transfected with the vector control or the RAG1/RAG2 expression vectors. Because HDR frequencies are only 0.026% for DRGFP-SE-containing cells and 0.073% for DRGFP-CE-containing cells, the bulk of the 1.1-kb PCR fragment is inferred to arise from NHEJ, giving rise to signal joint and coding joint formation, respectively. PCR fragments were electrophoresed and probed with a *GFP* fragment. C. Quantitation of the PCRs is shown in panel B. The 1.1-kb fragment from NHEJ and HDR was quantitated relative to the unrearranged 1.5-kb fragment and then adjusted using the standard curve. D. RAG-generated DSBs are repaired by SSA at low frequency compared to DSBs generated by I-SceI. Short (15-min) and long (16-h) exposures of the PCR-Southern blot are shown for the I-SceI transfection; the long exposure is shown for the other transfections.

the 1.5-kb fragment and a readily detectable 1.1-kb fragment. For cells containing the DRGFP-SE reporter, approximately 1.7% of DNA was estimated to be repaired by NHEJ and HDR combined; for cells containing the DRGFP-CE reporter, approximately 3.0% of the reporter was estimated to be repaired by these pathways. Quantification by Southern blotting gave similar results (data not shown). The almost twofold-higher level for the DRGFP-CE reporter compared with the DRGFP-SE reporter appears to account for much of the difference in HDR levels obtained with the two reporters (Fig. 1C), suggesting that the DRGFP-CE reporter is somewhat more efficiently cleaved than the DRGFP-SE reporter, rather than that blunt signal ends are less recombinogenic than hairpin coding ends. Considering the level of GFP^+ cells obtained for cells containing the two reporters (Fig. 1C), these results indicate that the frequency of NHEJ is substantially higher ($\geq$40-fold) than that of HDR for the repair of the RAG-generated DSBs.

In lymphocytes, V(D)J recombination is restricted to the G_0/G_1 phases of the cell cycle as a result of degradation of RAG2 at the G_1/S boundary caused by cyclin A/CDK2-dependent phosphorylation at residue T490 (18, 21, 25). Since HDR is expected to be most frequent during S/G_2, in part because proteins such as Rad51 are preferentially expressed during these cell cycle phases (51), we sought to determine whether RAG-induced HDR was inefficient as a result of a cell cycle-dependent loss of RAG2. For this, we utilized the RAG2-T490A mutant, which does not undergo cyclin-dependent phosphorylation (18, 21). Comparable levels of HDR were observed in cells containing the DRGFP-CE reporter after transient expression of RAG1/RAG2 or RAG1/RAG2-T490A (data not shown).

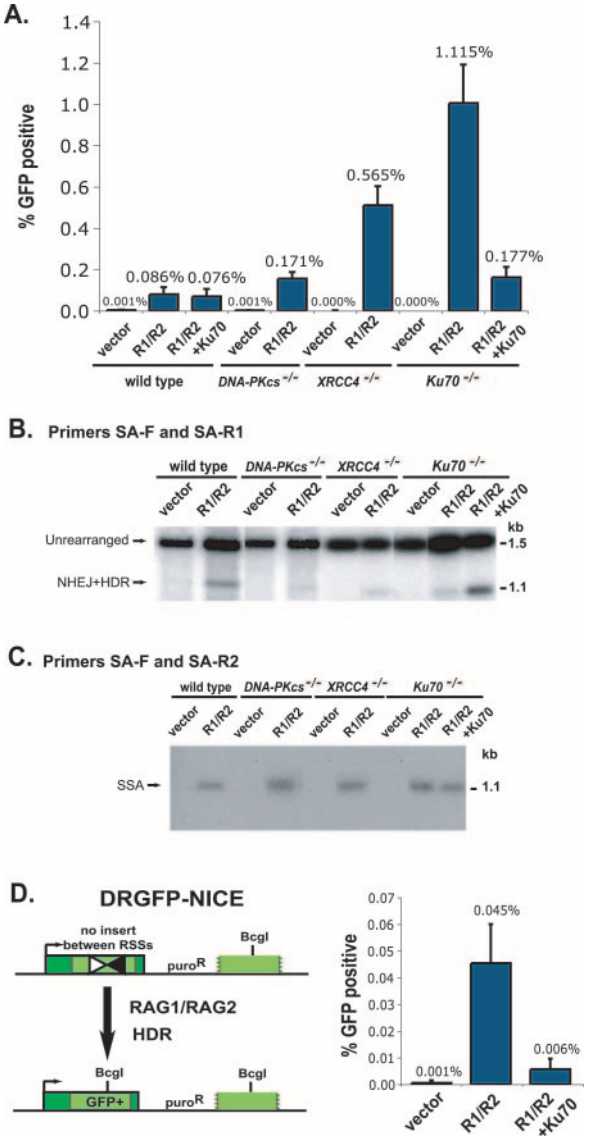

FIG. 3. RAG-induced HDR is increased in NHEJ-deficient cells. A. Using the DRGFP-CE reporter, HDR as measured by the percentage of GFP$^+$ cells is compared between wild-type (two clones), *Ku70*$^{-/-}$ (three clones), *DNA-PKcs*$^{-/-}$ (two clones), and *XRCC4*$^{-/-}$ (four clones) cells after transfection of the RAG1 and RAG2 expression vectors (R1/R2) or the empty expression vector. The increase in HDR is greatest for the *Ku70*$^{-/-}$ cells but is suppressed by coexpression of RAG1/RAG2 and Ku70. The differences in the percentage of GFP$^+$ cells between wild-type cells and the three NHEJ mutants are statistically significant (*Ku70*$^{-/-}$, $P < 0.00001$; *DNA-PKcs*$^{-/-}$, $P < 10^{-7}$; *XRCC4*$^{-/-}$, $P < 10^{-13}$), as is the difference between *Ku70*$^{-/-}$ and *XRCC4*$^{-/-}$ cells ($P < 0.0001$). B. NHEJ giving rise to coding joint formation is decreased in the mutant cell lines. Despite the increase in HDR, the level of combined DSB repair from NHEJ and HDR, as assayed by PCR with primers SA-F and SA-R1 to generate a 1.1-kb fragment, is reduced in the NHEJ mutants. In *Ku70*$^{-/-}$ cells, the level of the 1.1-kb repair fragment is restored by cotransfection with the Ku70 expression vector. Because HDR is increased in the NHEJ mutants, the decrease in the 1.1-kb PCR product indicates a significant reduction in NHEJ in the mutant cells. C. RAG-induced SSA is detected for each of the mutants and is not apparently increased in the NHEJ mutants. D. The DRGFP-NICE reporter is identical to the DRGFP-CE reporter except that it lacks an insert between the RSS elements. The overall level of HDR was much lower in *Ku70*$^{-/-}$ cells containing the DRGFP-NICE reporter than in *Ku70*$^{-/-}$ cells containing the DRGFP-CE reporter and is suppressed by Ku70 expression to extremely low levels. Results are derived from two targeted *Ku70*$^{-/-}$ cell lines. Symbols are as in Fig. 1.

SSA is also induced by the RAG recombinase. Using reporters similar to DR-GFP, it has previously been shown that a second repair pathway involving homology, SSA, can be used to repair an I-SceI-generated DSB in mammalian cells at a roughly similar frequency to HDR (44). To determine if RAG recombinase can also induce SSA, we physically analyzed DSB repair products using a PCR primer set (SA-F and SA-R2) that specifically amplifies the deletion product derived from SSA to give rise to a 1.1-kb fragment (Fig. 2A) (31). This same deletion product would also be obtained from an HDR pathway involving crossing over; however, crossovers have been measured in several systems to be rare outcomes of HDR, i.e., <2% of HDR events (5, 39, 43), so a significant contribution of crossovers to deletion events is unlikely. We have also previously ruled out significant contributions from more-complicated HDR events to the 1.1-kb PCR fragment (31).

From cells containing the DRGFP-SE and DRGFP-CE reporters, we obtained the 1.1-kb PCR fragment after RAG1/RAG2 expression, but not after transfection of the vector control, indicating that SSA is an additional pathway for the repair of RAG-generated breaks (Fig. 2D). As with HDR and NHEJ, SSA was estimated to be on average twofold higher in cells containing the DRGFP-CE reporter compared with cells containing the DRGFP-SE reporter, consistent with the interpretation that the DRGFP-CE reporter is somewhat more efficiently cleaved than the DRGFP-SE reporter. The level of the SSA product obtained after RAG1/RAG2 expression was compared to that obtained after I-SceI expression in cells containing the DR-GFP reporter (Fig. 2D). In multiple experiments, the SSA product was obtained at estimated 80- and 150-fold-higher levels after I-SceI expression in DR-GFP-containing cells than after RAG1/RAG2 expression in the DRGFP-CE- and DRGFP-SE-containing cells, respectively (Fig. 2C and data not shown). These results indicate that SSA, like HDR, constitutes a small fraction of the repair of RAG-generated breaks.

NHEJ components suppress RAG-induced HDR. Given that NHEJ overwhelmingly predominates in the repair of RAG-generated breaks in our reporters, we sought to determine whether the NHEJ components affect the level of repair by alternative pathways. For this, the DRGFP-CE reporter was targeted to the *hprt* locus in *Ku70*$^{-/-}$, *DNA-PKcs*$^{-/-}$, and *XRCC4*$^{-/-}$ ES cells (9, 10, 12) (data not shown). As with wild-type cells, very few GFP$^+$ cells were obtained among the NHEJ-deficient cells in the absence of RAG1/RAG2 expression (Fig. 3A). After RAG1/RAG2 expression, GFP$^+$ cells were obtained from all of the mutant cell lines. Importantly, the level of HDR was significantly higher in the mutant cells compared with wild-type cells. The increase in HDR was largest in *Ku70*$^{-/-}$ cells; compared to wild-type cells, HDR was increased 13-fold in *Ku70*$^{-/-}$ cells, 6.6-fold in *XRCC4*$^{-/-}$ cells, and 2-fold in *DNA-PKcs*$^{-/-}$ ES cells. Similar results were observed for *Ku70*$^{-/-}$ and *XRCC4*$^{-/-}$ cells with a single copy of the DRGFP-CE reporter randomly integrated (*hprt*$^+$/*puro*^{R})

into the genome (data not shown), arguing that the increase in HDR in the NHEJ mutants was not locus specific. Transient expression of Ku70 in the *Ku70*$^{-/-}$ cells substantially reduced HDR (6.3-fold) while having little effect in wild-type cells (Fig. 3A), verifying the Ku70 dependence of the HDR enhancement.

We also tested RAG-induced HDR and the effect of *Ku70* mutation using a precursor to the DRGFP-CE reporter, termed DRGFP-NICE, in which the two RSS elements are adjacent to each other rather than being separated by a spacer (Fig. 3D). The level of HDR was extremely low with this substrate both in Ku70-complemented (0.006%) and uncomplemented (0.045%), *Ku70*$^{-/-}$ cells (Fig. 3D), suggesting that the RAG recombinase inefficiently cleaves this substrate due to the close proximity of the two elements. The overall ratios of HDR were similar between the uncomplemented *Ku70*$^{-/-}$ cells and the Ku70-complemented cells (7.5-fold), again indicating that Ku70 suppresses HDR of RAG-generated breaks.

Other pathways of repair in NHEJ-deficient cells. Since V(D)J recombination is severely compromised by NHEJ deficiency (6), we expected that V(D)J recombination in our reporters would be markedly reduced in the NHEJ-deficient cell lines. To test this, we used the primer pair SA-F and SA-R1 to amplify NHEJ junctions (i.e., coding joints) from cells containing the DRGFP-CE reporter and compared the intensity of the amplification product to the product from the unrearranged reporter. We found that the intensity of the 1.1-kb fragment, which results from both the NHEJ junctions and the HDR product, was noticeably reduced in NHEJ mutant cells compared with wild-type cells, although faint bands were still visible that were not present in the absence of RAG expression (Fig. 3B). Transient coexpression of Ku70 and RAG1/RAG2 in the *Ku70*$^{-/-}$ cells restored the level of this fragment to wild-type levels. As HDR was increased in each of the mutants, the decreased intensity of the 1.1-kb fragment indicates that the ratio of HDR to NHEJ was markedly shifted (i.e., increased) in the NHEJ-deficient cell lines.

RAG-induced SSA was also examined in the NHEJ mutant cells. The 1.1-kb PCR product derived from SSA was detected in each of the mutants (Fig. 3C). The levels of the PCR fragment were roughly similar to that found in wild-type cells and, in addition, complementation of the *Ku70*$^{-/-}$ cells by coexpression of Ku70 and RAG1/RAG2 did not detectably alter the levels of this fragment (Fig. 3C). Thus, RAG-induced SSA was not noticeably suppressed by NHEJ factors.

We analyzed individual repair products from wild-type and *Ku70*$^{-/-}$ cells. Genomic DNA was cleaved with restriction enzymes that have sites within the spacer segment and then subjected to PCR with primers that flank the junction site (Fig. 4A). Resulting PCR fragments, which would be 0.8 kb from products with minor end modifications, were cloned and then screened for the presence of the BcgI restriction site to distinguish NHEJ products (i.e., coding joints) from HDR or SSA products. Almost all of the repair products from the wild-type cells were derived from NHEJ (46/50; 92%), whereas the majority of repair products from the *Ku70*$^{-/-}$ cells were derived from HDR or SSA (47/88; 53%), consistent with a shift in repair pathway usage in the NHEJ mutant cells ($P < 0.00001$).

Several of the coding joints were sequenced. From wild-type

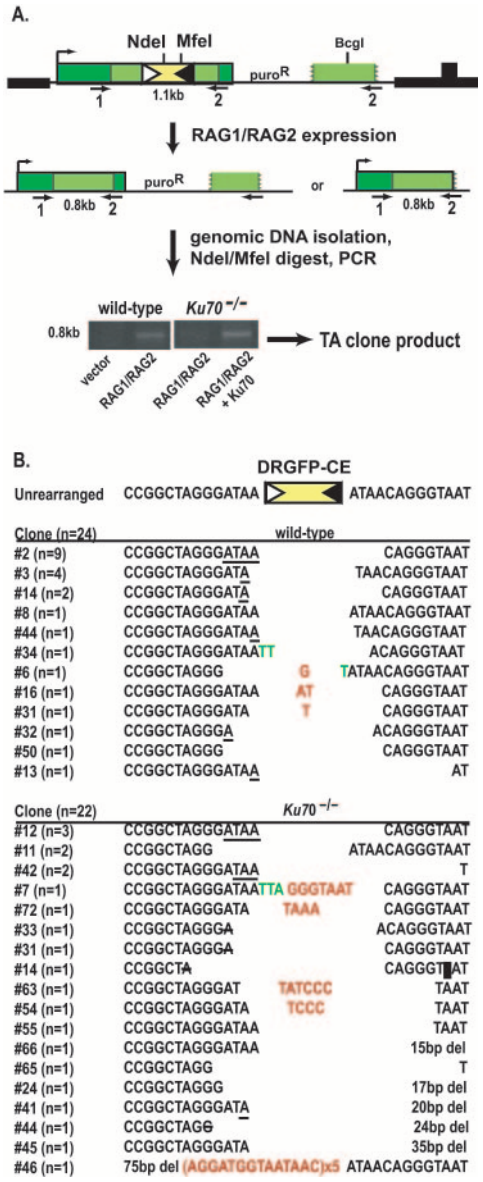

FIG. 4. Coding joints from wild-type and *Ku70*$^{-/-}$ cells. A. PCR strategy for cloning sequences resulting from RAG-induced NHEJ, HDR, or SSA in the DRGFP-CE reporter. Because of the large decrease in NHEJ in *Ku70*$^{-/-}$ cells, the amplified repair product is much lower than that from wild-type cells but is restored by Ku70 expression. Genomic DNA is predigested with NdeI and MfeI, which cleave within the unrearranged reporter. Primers 1 and 2 are used to amplify the RAG-induced repair products. The PCR product is inserted into a TA vector and transformed into *E. coli*. Plasmids containing an insert are subjected to BcgI digestion, which will cleave the insert if HDR or SSA occurs, but not if NHEJ occurs. DNA sequencing was performed on inserts derived from NHEJ. Symbols are as in Fig. 1. B. Ku70 deficiency alters the spectrum of coding joint products. Although some of the coding joints from *Ku70*$^{-/-}$ cells resemble those found in wild-type cells, most of the coding joints have larger deletions or other modifications. Microhomology (underlined), N nucleotides (red), P nucleotides (green), and an internally deleted nucleotide (black box) are indicated. Abbreviations: 1, DRGFP1; 2, DRGFP2.

cells, all but one junction (23/24; 96%) had deletions extending less than 5 bp on either side of the RAG-generated DSBs (Fig. 4B). P nucleotide and short N nucleotide insertions were evident in a few clones. In contrast, only 32% of junctions (7/22) from *Ku70*$^{-/-}$ cells had deletions extending less than 5 bp on either side of the RAG-generated DSB ($P < 0.00001$ compared to wild type); the remainder had larger deletions, extending up to 75 bp on one side. P nucleotides were evident, as were larger insertions of nucleotides, some of which may have been templated (e.g., a 7-bp insertion in clone 7 which is identical to the sequence 2 bp downstream). Overall, the junctions demonstrate characteristics similar to those previously reported for *Ku70*$^{-/-}$ cells using plasmid assays (12).

DISCUSSION

During V(D)J recombination, the repair of RAG-generated DSBs by the classical NHEJ pathway contributes much of the antigen receptor diversity necessary for immune system function (6, 11). We have determined that chromosomal breaks generated by the RAG recombinase can be repaired by pathways other than NHEJ in mouse ES cells, although repair by alternative pathways occurs at a significantly lower frequency than NHEJ. HDR was estimated to be utilized at a ≥40-fold-lower frequency than NHEJ for both the coding end and signal end reporters. SSA was more difficult to precisely quantify, but it was estimated to occur at a comparable or lower frequency than HDR. As expected, coding joint formation was impaired in cells deficient for the classical NHEJ components Ku70, XRCC4, and DNA-PKcs. Concomitant with this, RAG-induced HDR was increased in each of the NHEJ-deficient cell lines, including cells lacking DNA-PKcs. Among the NHEJ mutants, the largest increase in HDR occurred in *Ku70*$^{-/-}$ cells. Thus, RAG-generated DSBs are typically channeled into the NHEJ pathway and the absence of NHEJ components allows for repair by the alternative HDR pathway.

The RAG recombinase has recently been postulated to directly "shepherd" DSBs into NHEJ, since joining-deficient RAG proteins display enhanced HDR (17). Given the low frequency of HDR in wild-type cells, our results are consistent with a role for the RAG proteins in affecting repair pathway choice. However, our results also demonstrate a striking suppression of RAG-induced HDR by NHEJ pathway components. Loss of the Ku70 protein, in particular, caused a substantial shift toward HDR, such that the level of HDR in *Ku70*$^{-/-}$ cells approached the estimated level of coding joint formation in wild-type cells (~1% versus 3%, respectively), and as well approached the level of HDR found in wild-type cells after I-SceI cleavage (~1% versus 2%, respectively).

NHEJ pathway components also affect pathway choice in the repair of I-SceI-generated DSBs, with Ku70 having a stronger suppressive effect on I-SceI-induced HDR (fivefold) compared with other NHEJ components (35). It has been postulated that the Ku70/80 heterodimer prevents access of DNA ends to processing factors, such as the nuclease responsible for strand resection (19, 35, 49), and that the resulting increased access of ends to these factors in the *Ku70* mutant leads to a greater increase in HDR compared with loss of other NHEJ factors (35).

That RAG-induced HDR was also increased in *DNA-PKcs*$^{-/-}$ cells indicates that DNA-PKcs is not essential for hairpin opening at coding ends prior to HDR. Biochemical studies have indicated that DNA-PKcs forms a complex with and phosphorylates the Artemis protein, allowing Artemis to acquire the hairpin-opening activity which is essential for V(D)J recombination (27, 32). Consistent with this model, hairpin coding ends accumulate in both DNA-PKcs-deficient and Artemis-deficient thymocytes (9, 40, 41). A low level of coding joints is recovered from these cells (3, 9, 34, 40), however, implying the existence of alternative nicking activities, such as from the Mre11 complex. Direct analysis of hairpin metabolism in wild-type and *scid* cells also supports the existence of robust alternative pathways (20).

We expected that the regulation of the stability of RAG2, which is modulated by cell cycle-dependent phosphorylation, might also play a major role in restricting repair to NHEJ, by confining DSB formation to the G_1/G_0 stage of the cell cycle (18, 21, 25), when HDR frequency is generally considered to be low (47). Substitution of a phosphorylation-defective RAG2 (RAG2-T490A) did not, however, affect the level of HDR (data not shown). Phosphorylation has been shown to enhance ubiquitin-dependent degradation of RAG2 by promoting the transit of the protein from the nucleus to the cytoplasm (30). The requirement for T490 phosphorylation in ubiquitination is not absolute, however, implying that it is not the sole arbiter of RAG2 stability. Moreover, the ability of RAG-generated breaks to be efficiently channeled into the HDR pathway in *Ku70*$^{-/-}$ cells indicates that RAG-generated breaks have the potential to access the HDR machinery such that the regulation of RAG2 protein levels does not by itself regulate repair pathway choice.

Our results demonstrate that, like I-SceI-generated DSBs (22), RAG-generated breaks can be repaired by multiple pathways. Nevertheless, the results also suggest that the frequency of usage of the various pathways differs between the two types of breaks. In wild-type ES cells containing the reporter DR-GFP, we previously observed that I-SceI-generated chromosomal breaks are repaired by each of the three pathways (NHEJ, HDR, and SSA) at similar frequencies, with NHEJ being only a fewfold more frequent than either HDR or SSA (35, 44), rather than the ≥40-fold preference for NHEJ that we observed for RAG-generated DSBs. Direct comparison of the repair of I-SceI- and RAG-generated DSBs is complicated, however, because I-SceI-generated DSBs have the potential to be precisely rejoined (26), which allows for subsequent recleavage.

RAG-induced HDR was reported by Lee and colleagues (17), with remarkably similar levels of HDR observed with their hamster cell system as with our ES cell system. In this previous report, RAG-generated nicks rather than DSBs were postulated to be the instigators of most of the observed HDR events. The results we obtained are consistent with the induction of HDR by RAG-generated DSBs. For example, enhanced HDR was observed in the three different NHEJ mutants, each lacking proteins with distinct roles in DSB repair (24, 28). In addition, RAG-induced SSA was detected, which presumably reflects a DSB intermediate. Finally, we obtained a substantially higher frequency of HDR from the DRGFP-CE reporter, in which the two RSS elements are separated by a spacer, than with the DRGFP-NICE reporter, in which the two

RSS elements are adjacent to each other. RAG-generated nicks would be expected to lead to the same level of HDR in the DRGFP-NICE reporter or even enhanced HDR, since substantially less nonhomologous sequence would need to be removed from the broken end prior to HDR than with the DRGFP-CE reporter. Nonetheless, we cannot rule out the possibility that a portion of the HDR events that we detect are induced by RAG-generated nicks or nicks converted to DSBs, rather than frank DSBs.

In summary, RAG-generated chromosomal breaks can be repaired by multiple DSB repair pathways, although repair by V(D)J recombination using classical NHEJ components predominates. The biological significance of the alternative repair pathways is not certain, although they may provide a backup mechanism for the repair of RAG-generated breaks under some circumstances. The use of alternative pathways highlights the potential for DNA ends to "escape" from the normal control of the classical NHEJ components, which can lead to the misrepair of DSBs, genomic rearrangements, and tumorigenesis (7).

ACKNOWLEDGMENTS

We thank Stephen Desiderio (Johns Hopkins University School of Medicine) for providing RAG expression plasmids and Marty Gellert (NIH) for comments on the manuscript.

D.M.W. was supported by the Clinical Scholars Biomedical Research Training Program (NIH CA09512) and the Leukemia and Lymphoma Society (5415-05). This work was supported by NIH 54688 (M.J.).

REFERENCES

1. **Agrawal, A., and D. G. Schatz.** 1997. RAG1 and RAG2 form a stable postcleavage synaptic complex with DNA containing signal ends in V(D)J recombination. Cell **89:**43–53.
2. **Blackwell, T. K., B. A. Malynn, R. R. Pollock, P. Ferrier, L. R. Covey, G. M. Fulop, R. A. Phillips, G. D. Yancopoulos, and F. W. Alt.** 1989. Isolation of scid pre-B cells that rearrange kappa light chain genes: formation of normal signal and abnormal coding joints. EMBO J. **8:**735–742.
3. **Brown, M. L., and Y. Chang.** 2000. Metabolism of recombination coding ends in scid cells. J. Immunol. **164:**4135–4142.
4. **Difilippantonio, M. J., S. Petersen, H. T. Chen, R. Johnson, M. Jasin, R. Kanaar, T. Ried, and A. Nussenzweig.** 2002. Evidence for replicative repair of DNA double-strand breaks leading to oncogenic translocation and gene amplification. J Exp. Med. **196:**469–480.
5. **Dronkert, M. L., H. B. Beverloo, R. D. Johnson, J. H. Hoeijmakers, M. Jasin, and R. Kanaar.** 2000. Mouse RAD54 affects DNA double-strand break repair and sister chromatid exchange. Mol. Cell. Biol. **20:**3147–3156.
6. **Dudley, D. D., J. Chaudhuri, C. H. Bassing, and F. W. Alt.** 2005. Mechanism and control of V(D)J recombination versus class switch recombination: similarities and differences. Adv. Immunol. **86:**43–112.
7. **Ferguson, D. O., and F. W. Alt.** 2001. DNA double strand break repair and chromosomal translocation: lessons from animal models. Oncogene **20:**5572–5579.
8. **Frank, K. M., J. M. Sekiguchi, K. J. Seidl, W. Swat, G. A. Rathbun, H. L. Cheng, L. Davidson, L. Kangaloo, and F. W. Alt.** 1998. Late embryonic lethality and impaired V(D)J recombination in mice lacking DNA ligase IV. Nature **396:**173–177.
9. **Gao, Y., J. Chaudhuri, C. Zhu, L. Davidson, D. T. Weaver, and F. W. Alt.** 1998. A targeted DNA-PKcs-null mutation reveals DNA-PK-independent functions for KU in V(D)J recombination. Immunity **9:**367–376.
10. **Gao, Y., Y. Sun, K. M. Frank, P. Dikkes, Y. Fujiwara, K. J. Seidl, J. M. Sekiguchi, G. A. Rathbun, W. Swat, J. Wang, R. T. Bronson, B. A. Malynn, M. Bryans, C. Zhu, J. Chaudhuri, L. Davidson, R. Ferrini, T. Stamato, S. H. Orkin, M. E. Greenberg, and F. W. Alt.** 1998. A critical role for DNA end-joining proteins in both lymphogenesis and neurogenesis. Cell **95:**891–902.
11. **Gellert, M.** 2002. V(D)J recombination: RAG proteins, repair factors, and regulation. Annu. Rev. Biochem. **71:**101–132.
12. **Gu, Y., S. Jin, Y. Gao, D. Weaver, and F. Alt.** 1997. Ku70-deficient embryonic stem cells have increased ionizing radiosensitivity, defective DNA end-binding activity, and inability to support V(D)J. recombination. Proc. Natl. Acad. Sci. USA **94:**8076–8081.
13. **Hesse, J. E., M. R. Lieber, M. Gellert, and K. Mizuuchi.** 1987. Extrachromosomal DNA substrates in pre-B cells undergo inversion or deletion at immunoglobulin V-(D)-J joining signals. Cell **49:**775–783.
14. **Hiom, K., and M. Gellert.** 1998. Assembly of a 12/23 paired signal complex: a critical control point in V(D)J recombination. Mol. Cell **1:**1011–1019.
15. **Jeggo, P. A.** 1998. DNA breakage and repair. Adv. Genet. **38:**185–218.
16. **Johnson, R. D., and M. Jasin.** 2000. Sister chromatid gene conversion is a prominent double-strand break repair pathway in mammalian cells. EMBO J. **19:**3398–3407.
17. **Lee, G. S., M. B. Neiditch, S. S. Salus, and D. B. Roth.** 2004. RAG proteins shepherd double-strand breaks to a specific pathway, suppressing error-prone repair, but RAG nicking initiates homologous recombination. Cell **117:**171–184.
18. **Lee, J., and S. Desiderio.** 1999. Cyclin A/CDK2 regulates V(D)J recombination by coordinating RAG-2 accumulation and DNA repair. Immunity **11:**771–781.
19. **Lee, S. E., J. K. Moore, A. Holmes, K. Umezu, R. D. Kolodner, and J. E. Haber.** 1998. *Saccharomyces* Ku70, mre11/rad50 and RPA proteins regulate adaptation to G_2/M arrest after DNA damage. Cell **94:**399–409.
20. **Lewis, S.** 1994. P nucleotide insertions and the resolution of hairpin DNA structures in mammalian cells. Proc. Natl. Acad. Sci. USA **91:**1332–1336.
21. **Li, Z., D. I. Dordai, J. Lee, and S. Desiderio.** 1996. A conserved degradation signal regulates RAG-2 accumulation during cell division and links V(D)J recombination to the cell cycle. Immunity **5:**575–589.
22. **Liang, F., M. Han, P. J. Romanienko, and M. Jasin.** 1998. Homology-directed repair is a major double-strand break repair pathway in mammalian cells. Proc. Natl. Acad. Sci. USA **95:**5172–5177.
23. **Lieber, M. R., J. E. Hesse, S. Lewis, G. C. Bosma, N. Rosenberg, K. Mizuuchi, M. J. Bosma, and M. Gellert.** 1988. The defect in murine severe combined immune deficiency: joining of signal sequences but not coding segments in V(D)J recombination. Cell **55:**7–16.
24. **Lieber, M. R., Y. Ma, U. Pannicke, and K. Schwarz.** 2003. Mechanism and regulation of human non-homologous DNA end-joining. Nat. Rev. Mol. Cell Biol. **4:**712–720.
25. **Lin, W. C., and S. Desiderio.** 1993. Regulation of V(D)J recombination activator protein RAG-2 by phosphorylation. Science **260:**953–959.
26. **Lin, Y., T. Lukacsovich, and A. S. Waldman.** 1999. Multiple pathways for repair of DNA double-strand breaks in mammalian chromosomes. Mol. Cell. Biol. **19:**8353–8360.
27. **Ma, Y., U. Pannicke, K. Schwarz, and M. R. Lieber.** 2002. Hairpin opening and overhang processing by an Artemis/DNA-dependent protein kinase complex in nonhomologous end joining and V(D)J. recombination. Cell **108:**781–794.
28. **Meek, K., S. Gupta, D. A. Ramsden, and S. P. Lees-Miller.** 2004. The DNA-dependent protein kinase: the director at the end. Immunol. Rev. **200:**132–141.
29. **Miyazaki, J., S. Takaki, K. Araki, F. Tashiro, A. Tominaga, K. Takatsu, and K. Yamamura.** 1989. Expression vector system based on the chicken beta-actin promoter directs efficient production of interleukin-5. Gene **79:**269–277.
30. **Mizuta, R., M. Mizuta, S. Araki, and D. Kitamura.** 2002. RAG2 is down-regulated by cytoplasmic sequestration and ubiquitin-dependent degradation. J. Biol. Chem. **277:**41423–41427.
31. **Nakanishi, K., Y. G. Yang, A. J. Pierce, T. Taniguchi, M. Digweed, A. D. D'Andrea, Z. Q. Wang, and M. Jasin.** 2005. Human Fanconi anemia monoubiquitination pathway promotes homologous DNA repair. Proc. Natl. Acad. Sci. USA **102:**1110–1115.
32. **Pannicke, U., Y. Ma, K. P. Hopfner, D. Niewolik, M. R. Lieber, and K. Schwarz.** 2004. Functional and biochemical dissection of the structure-specific nuclease ARTEMIS. EMBO J. **23:**1987–1997.
33. **Paques, F., and J. E. Haber.** 1999. Multiple pathways of recombination induced by double-strand breaks in *Saccharomyces cerevisiae*. Microbiol. Mol. Biol. Rev. **63:**349–404.
34. **Paull, T. T., and M. Gellert.** 1999. Nbs1 potentiates ATP-driven DNA unwinding and endonuclease cleavage by the Mre11/Rad50 complex. Genes Dev. **13:**1276–1288.
35. **Pierce, A. J., P. Hu, M. Han, N. Ellis, and M. Jasin.** 2001. Ku DNA end-binding protein modulates homologous repair of double-strand breaks in mammalian cells. Genes Dev. **15:**3237–3242.
36. **Pierce, A. J., and M. Jasin.** 2005. Measuring recombination proficiency in mouse embryonic stem cells. Methods Mol. Biol. **291:**373–384.
37. **Pierce, A. J., R. D. Johnson, L. H. Thompson, and M. Jasin.** 1999. XRCC3 promotes homology-directed repair of DNA damage in mammalian cells. Genes Dev. **13:**2633–2638.
38. **Qiu, J. X., S. B. Kale, H. Yarnell Schultz, and D. B. Roth.** 2001. Separation-of-function mutants reveal critical roles for RAG2 in both the cleavage and joining steps of V(D)J recombination. Mol. Cell **7:**77–87.
39. **Richardson, C., M. E. Moynahan, and M. Jasin.** 1998. Double-strand break repair by interchromosomal recombination: suppression of chromosomal translocations. Genes Dev. **12:**3831–3842.
40. **Rooney, S., J. Sekiguchi, C. Zhu, H. L. Cheng, J. Manis, S. Whitlow, J. DeVido, D. Foy, J. Chaudhuri, D. Lombard, and F. W. Alt.** 2002. Leaky Scid

phenotype associated with defective V(D)J coding end processing in Artemis-deficient mice. Mol. Cell **10:**1379–1390.

41. **Roth, D. B., J. P. Menetski, P. B. Nakajima, M. J. Bosma, and M. Gellert.** 1992. V(D)J recombination: broken DNA molecules with covalently sealed (hairpin) coding ends in scid mouse thymocytes. Cell **70:**983–991.
42. **Stark, J. M., P. Hu, A. J. Pierce, M. E. Moynahan, N. Ellis, and M. Jasin.** 2002. ATP hydrolysis by mammalian RAD51 has a key role during homology-directed DNA repair. J. Biol. Chem. **277:**20185–20194.
43. **Stark, J. M., and M. Jasin.** 2003. Extensive loss of heterozygosity is suppressed during homologous repair of chromosomal breaks. Mol. Cell. Biol. **23:**733–743.
44. **Stark, J. M., A. J. Pierce, J. Oh, A. Pastink, and M. Jasin.** 2004. Genetic steps of mammalian homologous repair with distinct mutagenic consequences. Mol. Cell. Biol. **24:**9305–9316.
45. **Symington, L. S.** 2002. Role of RAD52 epistasis group genes in homologous recombination and double-strand break repair. Microbiol. Mol. Biol. Rev. **66:**630–670.
46. **Taccioli, G. E., G. Rathbun, E. Oltz, T. Stamato, P. A. Jeggo, and F. W. Alt.** 1993. Impairment of V(D)J recombination in double-strand break repair mutants. Science **260:**207–210.
47. **Takata, M., M. S. Sasaki, E. Sonoda, C. Morrison, M. Hashimoto, H. Utsumi, Y. Yamaguchi-Iwai, A. Shinohara, and S. Takeda.** 1998. Homologous recombination and non-homologous end-joining pathways of DNA double-strand break repair have overlapping roles in the maintenance of chromosomal integrity in vertebrate cells. EMBO J. **17:**5497–5508.
48. **Tsai, C. L., A. H. Drejer, and D. G. Schatz.** 2002. Evidence of a critical architectural function for the RAG proteins in end processing, protection, and joining in V(D)J recombination. Genes Dev. **16:**1934–1949.
49. **Van Dyck, E., A. Z. Stasiak, A. Stasiak, and S. C. West.** 1999. Binding of double-strand breaks in DNA by human Rad52 protein. Nature **398:**728–731.
50. **Verkaik, N. S., R. E. Esveldt-van Lange, D. van Heemst, H. T. Bruggenwirth, J. H. Hoeijmakers, M. Z. Zdzienicka, and D. C. van Gent.** 2002. Different types of V(D)J recombination and end-joining defects in DNA double-strand break repair mutant mammalian cells. Eur. J. Immunol. **32:**701–709.
51. **Yamamoto, A., T. Taki, H. Yagi, T. Habu, K. Yoshida, Y. Yoshimura, K. Yamamoto, A. Matsushiro, Y. Nishimune, and T. Morita.** 1996. Cell cycle-dependent expression of the mouse Rad51 gene in proliferating cells. Mol. Gen. Genet. **251:**1–12.
52. **Yarnell Schultz, H., M. A. Landree, J. X. Qiu, S. B. Kale, and D. B. Roth.** 2001. Joining-deficient RAG1 mutants block V(D)J recombination in vivo and hairpin opening in vitro. Mol. Cell **7:**65–75.
53. **Zhu, C., K. D. Mills, D. O. Ferguson, C. Lee, J. Manis, J. Fleming, Y. Gao, C. C. Morton, and F. W. Alt.** 2002. Unrepaired DNA breaks in p53-deficient cells lead to oncogenic gene amplification subsequent to translocations. Cell **109:**811–821.